Science Advances
AAAS

advances.sciencemag.org/cgi/content/full/5/5/eaav7999/DC1

Supplementary Materials for

Control of antiviral innate immune response by protein geranylgeranylation

Shigao Yang, Alfred T. Harding, Catherine Sweeney, David Miao, Gregory Swan, Connie Zhou, Zhaozhao Jiang, Katherine A. Fitzgerald, Gianna Hammer, Martin O. Bergo, Heather K. Kroh, D. Borden Lacy, Chunxiang Sun, Michael Glogauer, Loretta G. Que, Nicholas S. Heaton, Donghai Wang*

*Corresponding author. Email: donghai.wang@duke.edu

Published 29 May 2019, *Sci. Adv.* **5**, eaav7999 (2019)
DOI: 10.1126/sciadv.aav7999

This PDF file includes:

Supplementary Material

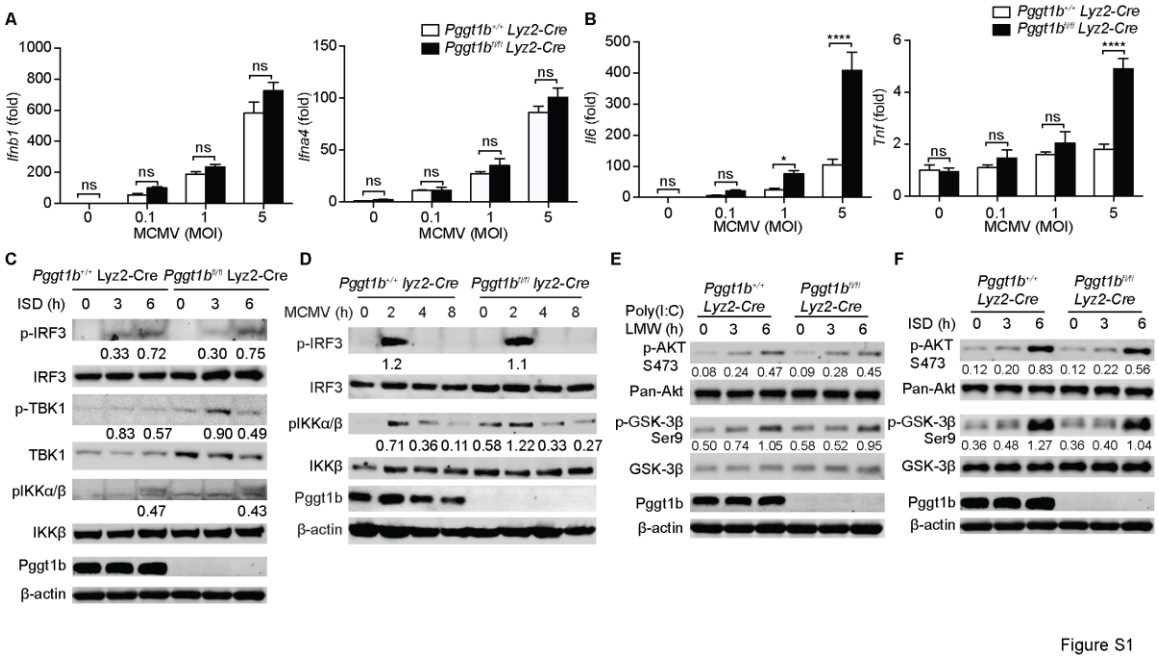

Figure S1

Fig. S1. Protein geranylgeranylation has no effect on DNA virus–induced antiviral innate immune response. (**A** and **B**) Quantitative RT-PCR analysis of transcript abundance of *Ifnb1*, *Ifna4*, *Il6* and *Tnf* in *Pggt1b*$^{+/+}$ *Lyz2-Cre* and *Pggt1b*$^{fl/fl}$ Lyz2-Cre BMDMs 4 h following infection with mouse cytomegalovirus (MCMV). (**C** and **D**) Immunoblot analysis of phosphorylated (p-) or total IRF3, TBK1, IKK and Pggt1b or β-actin in *Pggt1b*$^{+/+}$ *Lyz2-Cre* and *Pggt1b*$^{fl/fl}$ *Lyz2-Cre* BMDMs transfected with ISD (**C**) or infected with mouse Cytomegalovirus (MCMV, 1 MOI) (**D**). (**E** and **F**) Immunoblot with phosphor-Akt S473, pan-Akt, phosphor-Gsk3β Ser9, and Gsk3β antibody of BMDMs cell lysates transfected with poly I:C LMW (**E**) or ISD (**F**); Numbers below lanes indicate densitometry of phosphorylated AKT S473 or GSK-3β relative to that of total AKT S473 or GSK-3β respectively. *p: ＜0.05, ****p: ＜0.0001 (two-way ANOVA). Data are representative of three independent biological experiments.

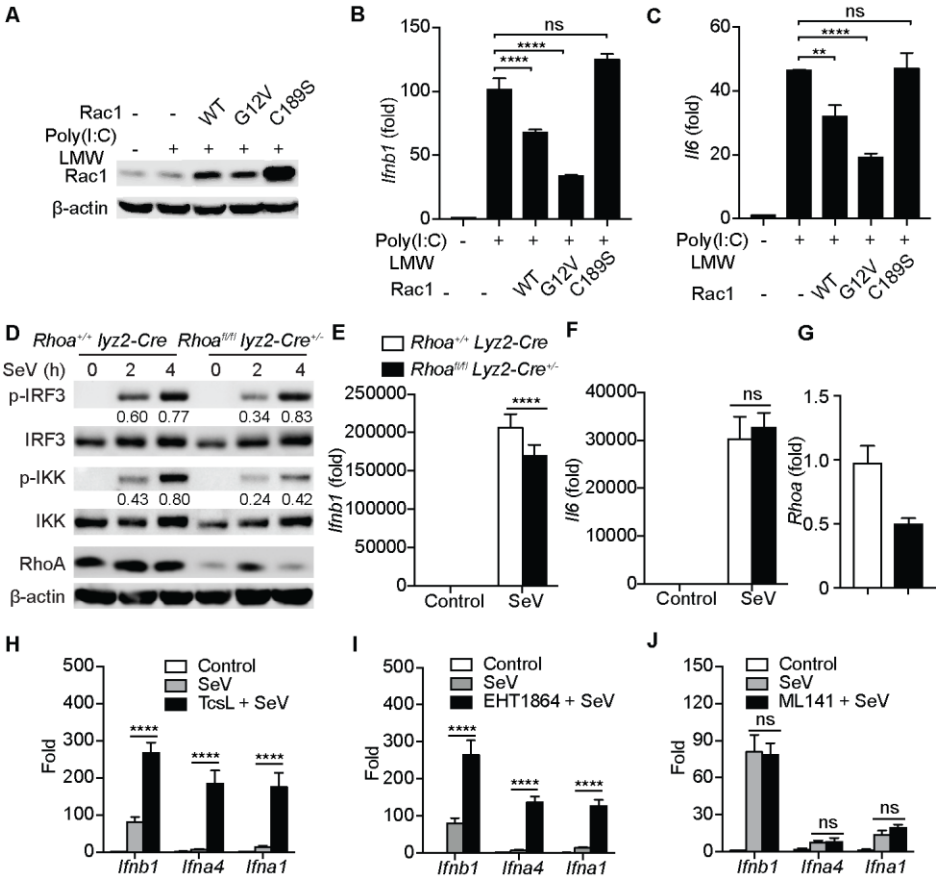
A
Rac1 - - WT G12V C189S
Poly(I:C) - + + + +
LMW Rac1
β-actin
B
Ifnb1 (fold)
ns
****
****
Poly(I:C) - + + + +
LMW Rac1 - - WT G12V C189S
C
Il6 (fold)
ns
****
**
Poly(I:C) - + + + +
LMW Rac1 - - WT G12V C189S
D
Rhoa+/+ lyz2-Cre Rhoafl/fl lyz2-Cre+/-
SeV (h) 0 2 4 0 2 4
p-IRF3
0.60 0.77 0.34 0.83
IRF3
p-IKK
0.43 0.80 0.24 0.42
IKK
RhoA
β-actin
E
Rhoa+/+ Lyz2-Cre
Rhoafl/fl Lyz2-Cre+/-
Ifnb1 (fold)
****
Control SeV
F
Il6 (fold)
ns
Control SeV
G
Rhoa (fold)
H
Control
SeV
TcsL + SeV
Fold
****
Ifnb1 Ifna4 Ifna1
I
Control
SeV
EHT1864 + SeV
Fold
****
Ifnb1 Ifna4 Ifna1
J
Control
SeV
ML141 + SeV
Fold
ns
Ifnb1 Ifna4 Ifna1

Figure S2

Fig. S2. Rac1 but not RhoA or Cdc42 suppresses MAVS signaling in a protein geranylgeranylation–dependent manner. (**A** to **C**) Immunoblot of Rac1 (**A**) and *Ifnb1* and *Il6* transcript abundance (**B** and **C**) in MEFs stably expressing wild-type (WT), constitutive active form (G12V), or C189S mutant *Rac1* after transfection with 1 μg/mL of poly (I:C) LMW for 4 h. (**D**) Immunoblot of phospho-IRF3 and phospho-IKK in cell lysates of *Rhoa*$^{+/+}$ *lyz2-Cre* and *Rhoa*$^{fl/fl}$ *lyz2-Cre*$^{+/-}$ BMDMs after SeV infection. (**E** to **G**) Quantitative RT-PCR analysis of transcript abundance of *Ifnb1*, *Il6* and *Rhoa* in *Rhoa*$^{+/+}$ *lyz2-Cre* and *Rhoa*$^{fl/fl}$ *lyz2-Cre*$^{+/-}$ BMDMs 4 h after SeV infection. (**H** to **J**) Quantitative RT-PCR analysis of transcript abundance of *Ifnb1*, *Ifna4* and *Ifna1* in BMDMs pre-treated with 100 ng/mL TcsL toxin (**H**), 20 μM Rac inhibitor EHT1864 (**I**), or 20 μM Cdc42 inhibitor ML141 (**J**), followed by infection with SeV for 4 h. **p: ＜ 0.01, ****p: ＜0.0001 (two-way ANOVA). Data are representative of three independent experiments.

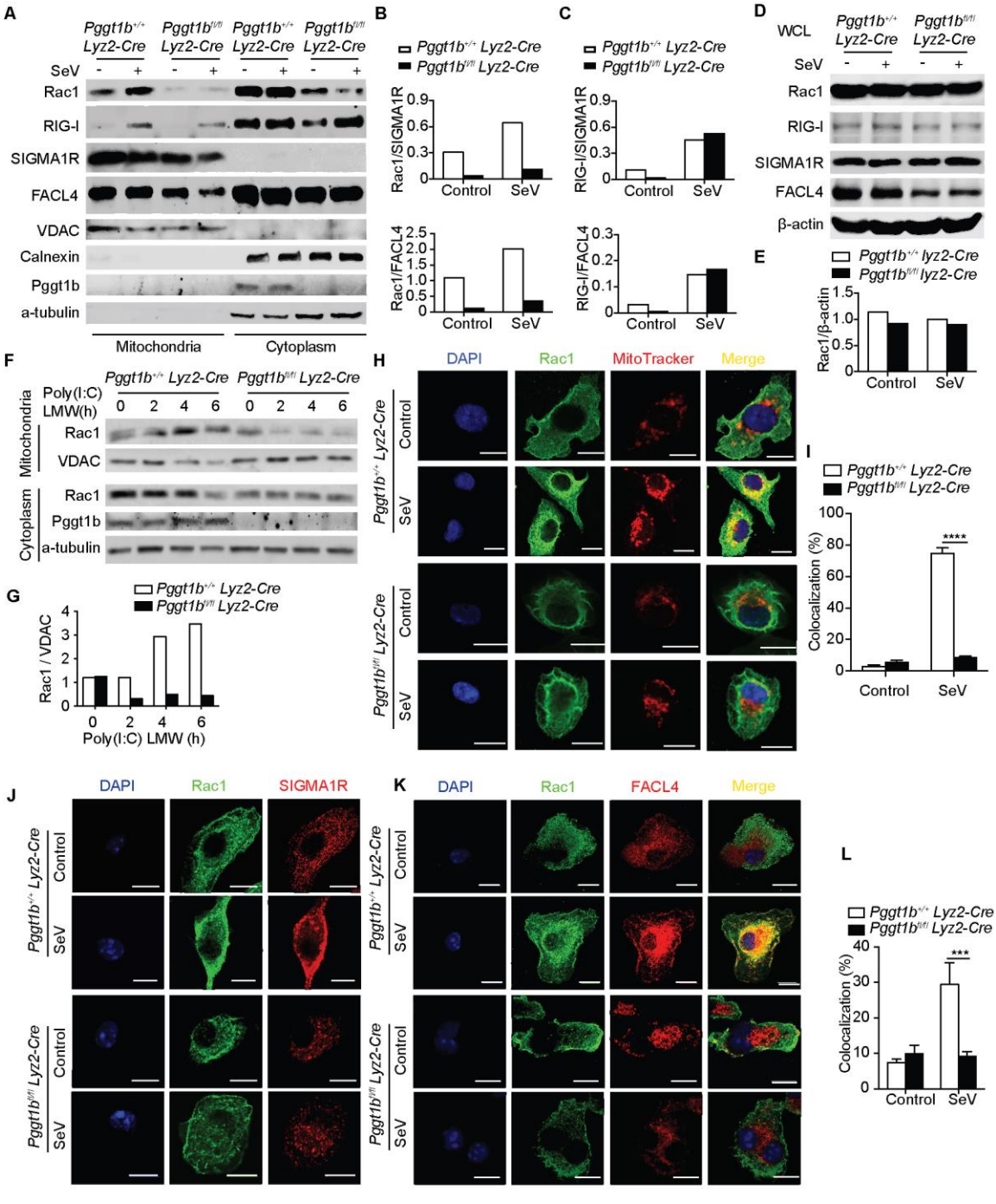
A
Pggt1b+/+ Lyz2-Cre
Pggt1bf/f Lyz2-Cre
SeV
Rac1
RIG-I
SIGMA1R
FACL4
VDAC
Calnexin
Pggt1b
a-tubulin
Mitochondria
Cytoplasm
B
Rac1/SIGMA1R
Rac1/FACL4
Control
SeV
C
RIG-I/SIGMA1R
RIG-I/FACL4
D
WCL
β-actin
E
Rac1/β-actin
F
Poly(I:C) LMW(h)
0 2 4 6
G
Rac1 / VDAC
Poly(I:C) LMW (h)
H
DAPI
Rac1
MitoTracker
Merge
I
Colocalization (%)
****
J
SIGMA1R
K
FACL4
L
***

Figure S3

Fig. S3. Protein geranylgeranylation targets Rac1 to MERC ER membranes upon RLR engagement. (**A**) Immunoblot of crude mitochondria and cytoplasm fractions from *Pggt1b*$^{+/+}$ Lyz2-Cre and *Pggt1b*$^{fl/fl}$ Lyz2-Cre BMDMs after SeV infection. (**B** and **C**) Abundance of Rac1 or RIG-I relative to MERC-ER marker SIGMA1R or FACL4 were quantitated using ImageJ. (**D**) Immunoblot of whole cell lysates (WCL) from *Pggt1b*$^{+/+}$ Lyz2-Cre and *Pggt1b*$^{fl/fl}$ Lyz2-Cre BMDMs infected with SeV. (**E**) Densitometry of Rac1 relative to that of β-actin in WCL of (**D**). (**F**) Immunoblot of crude mitochondria and cytoplasm fractions from *Pggt1b*$^{+/+}$ *Lyz2-Cre* and *Pggt1b*$^{fl/fl}$ Lyz2-Cre BMDMs transfected with poly (I:C) LMW. (**G**) Abundance of Rac1 relative to VDAC in (**F**) was quantitated using ImageJ. (**H**) Confocal microscopy of Rac1 in *Pggt1b*$^{+/+}$ *Lyz2-Cre* and *Pggt1b*$^{fl/fl}$ *Lyz2-Cre* BMDMs after SeV infection. MitoTracker was used to label mitochondria. Scale bar is 10 μm. (**I**) The percentage of colocalization was calculated using the ImageJ Software from at least 50 cells randomly selected from the immunostaining slides (**H**). (**J**) Single channels of DAPI, Rac1 and SIGMAR1 for Fig. 2**I**. (**K** and **L)** Confocal microscopy of immunofluorescent staining of Rac1 (green) and FACL4 (red) in *Pggt1b*$^{+/+}$ Lyz2-Cre and *Pggt1b*$^{fl/fl}$ Lyz2-Cre BMDMs after SeV infection; Cells were counterstained with DAPI (blue); scale bar is 10 μm (**K**); (**L**) The percentage of colocalization was calculated using the ImageJ software from at least 50 cells randomly selected from the immunostaining slides (**K**); ***p: $<$ 0.001, ****p: $<$ 0.0001 (two-way ANOVA). Data are representative of three independent experiments.

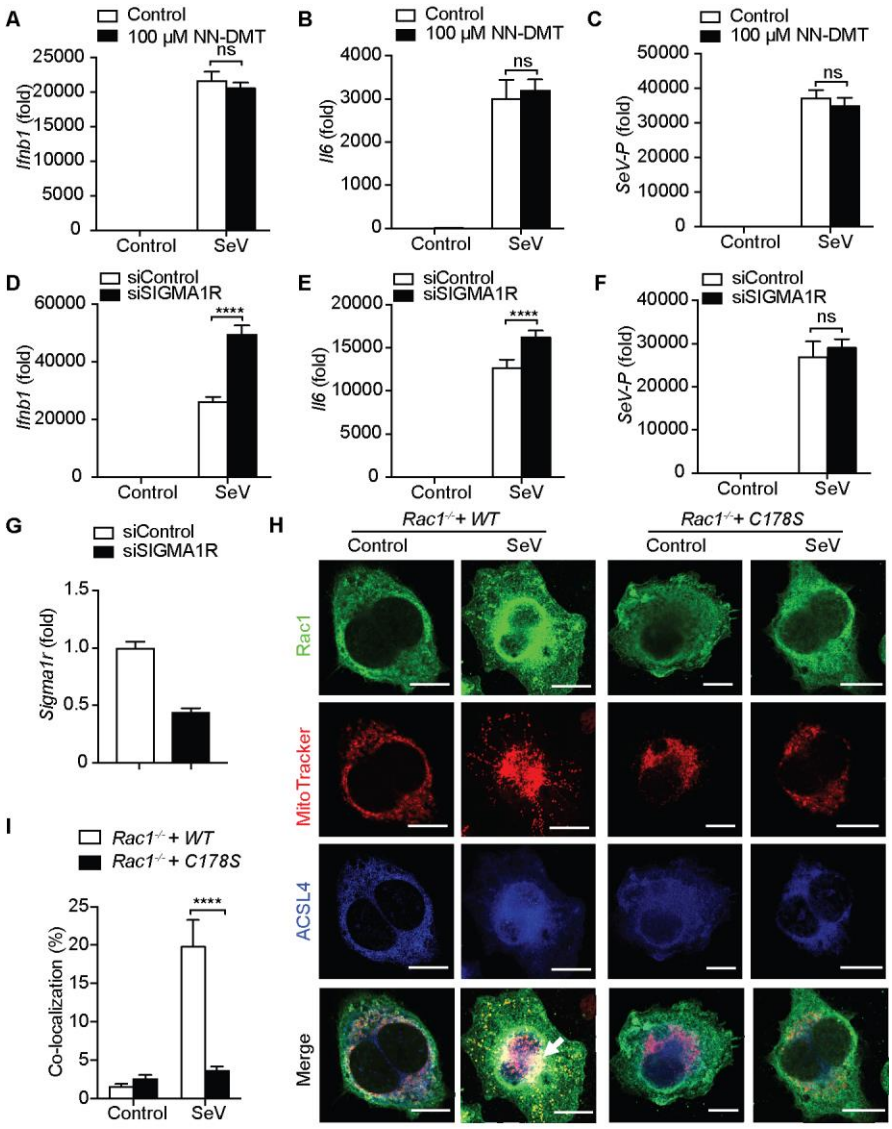
A
Control
100 μM NN-DMT
ns
Ifnb1 (fold)
25000
20000
15000
10000
5000
0
Control
SeV
B
Control
100 μM NN-DMT
ns
Il6 (fold)
4000
3000
2000
1000
0
Control
SeV
C
Control
100 μM NN-DMT
ns
SeV-P (fold)
50000
40000
30000
20000
10000
0
Control
SeV
D
siControl
siSIGMA1R
****
Ifnb1 (fold)
60000
40000
20000
0
Control
SeV
E
siControl
siSIGMA1R
****
Il6 (fold)
20000
15000
10000
5000
0
Control
SeV
F
siControl
siSIGMA1R
ns
SeV-P (fold)
40000
30000
20000
10000
0
Control
SeV
G
siControl
siSIGMA1R
Sigma1r (fold)
1.5
1.0
0.5
0
H
Rac1−/− + WT
Rac1−/− + C178S
Control
SeV
Control
SeV
Rac1
MitoTracker
ACSL4
Merge
I
Rac1−/− + WT
Rac1−/− + C178S
****
Co-localization (%)
25
20
15
10
5
0
Control
SeV

Figure S4

Fig. S4. Chaperon but not the signaling function of SIGMA1R and Rac1 palmitoylation is important for anchoring Rac1 to MERC ER membranes. (**A** to **C**) Quantitative RT-PCR analysis of transcript abundance of *Ifnb1*, *Il6* and *SeV-P* in BMDMs pre-treated with 100 μM NN-DMT for 1 h, followed by SeV infection. (**D** to **G**) Quantitative RT-PCR analysis of transcript abundance of *Ifnb1*, *Il6*, *SeV-P* and *Sigma1r* in BMDMs transfected with 100 nM Sigma1r siRNA or scramble siRNA for 48 h, followed by SeV infection; ****p: ＜0.0001 (two-way ANOVA). (**H** and **I**) Confocal microscopy of colocalization of WT and C178S mutant form of Rac1 (green) together with MitoTracker (Red) and FACL4 (blue) in *Rac1*$^{-/-}$ iBMDMs reconstituted with WT or C178S Rac1, scale bar is 10 μm (**H**); (**I**) The percentage of colocalization among Rac1, MitoTracker and FACL4 was calculated using ImageJ (**H**); ****p: ＜ 0.0001 (two-way ANOVA). Data represent the average and standard error of three independent experiments.

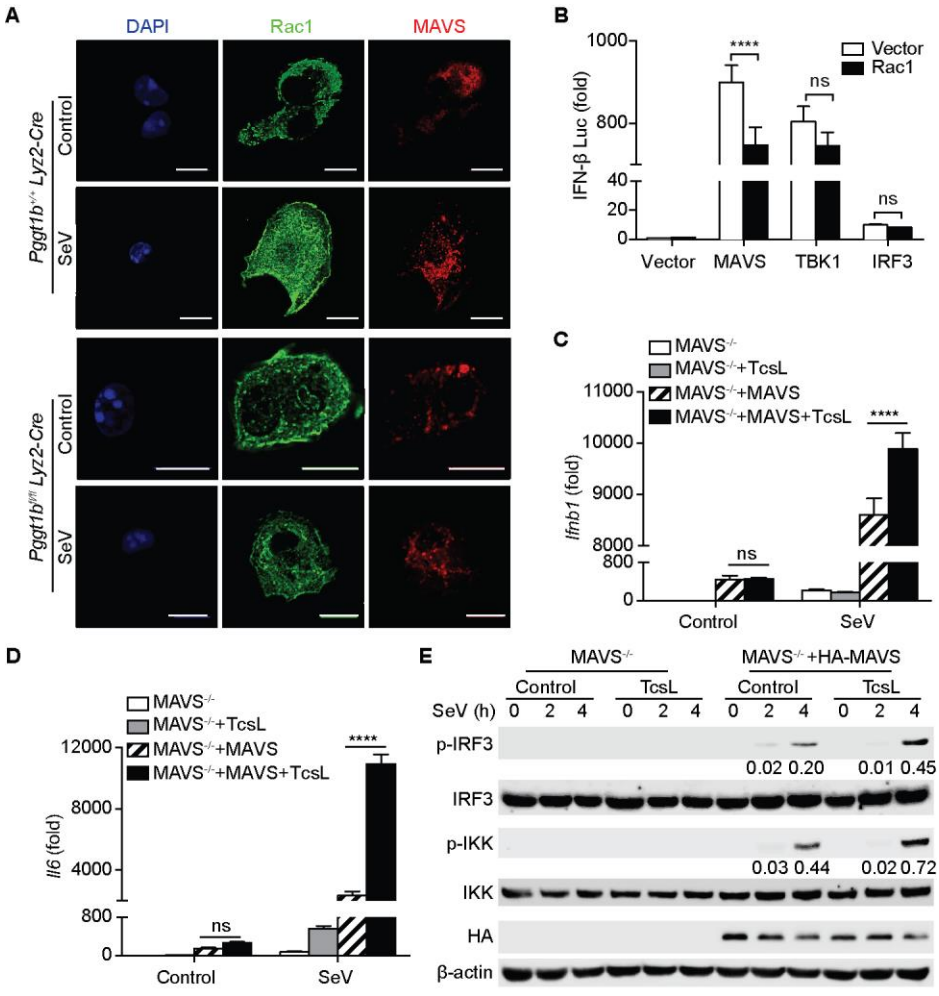
A
DAPI
Rac1
MAVS
Pggt1b+/+ Lyz2-Cre
Pggt1bf/f Lyz2-Cre
Control
SeV
B
IFN-β Luc (fold)
Vector
Rac1
****
ns
Vector
MAVS
TBK1
IRF3
C
MAVS-/-
MAVS-/-+TcsL
MAVS-/-+MAVS
MAVS-/-+MAVS+TcsL
Ifnb1 (fold)
Control
SeV
D
Il6 (fold)
E
MAVS-/-
MAVS-/- +HA-MAVS
Control
TcsL
SeV (h)
p-IRF3
0.02 0.20
0.01 0.45
IRF3
p-IKK
0.03 0.44
0.02 0.72
IKK
HA
β-actin

Figure S5

Fig. S5. Rac1 directly engages MAVS signalosome and inhibits MAVS signaling in a protein geranylgeranylation–dependent manner. (**A**) Single channels of DAPI, Rac1 and MAVS for Fig. 3**B**. (**B**) Luciferase activity 24 hours after IFNβ-luciferase reporter, MAVS, TBK1 or IRF3 encoding plasmid were transfected together with wild-type Rac1 expressing plasmid into 293 cells. (**C** and **D**) Quantitative RT-PCR analysis of *Ifnb1* and *Il6* in *MAVS*$^{-/-}$ iBMDMs or *MAVS*$^{-/-}$ iBMDMs reconstituted with wild-type MAVS pretreated with TcsL followed by SeV infection; ****p: ＜0.0001 (two-way ANOVA). (**E**) Immunoblot of phospho-IRF3 and phospho-IKK in cell lysates of immortalized *MAVS*$^{-/-}$ iBMDMs stably reconstituted with HA-tagged Mavs (MAVS$^{-/-}$ + HA-MAVS) pre-treated with TcsL followed by infection with SeV; Numbers below lanes indicate densitometry of phosphorylated IRF3 or IKK relative to that of total IRF3 or IKK respectively. ****p: ＜0.0001 (two-way ANOVA). Data are representative of three independent experiments.

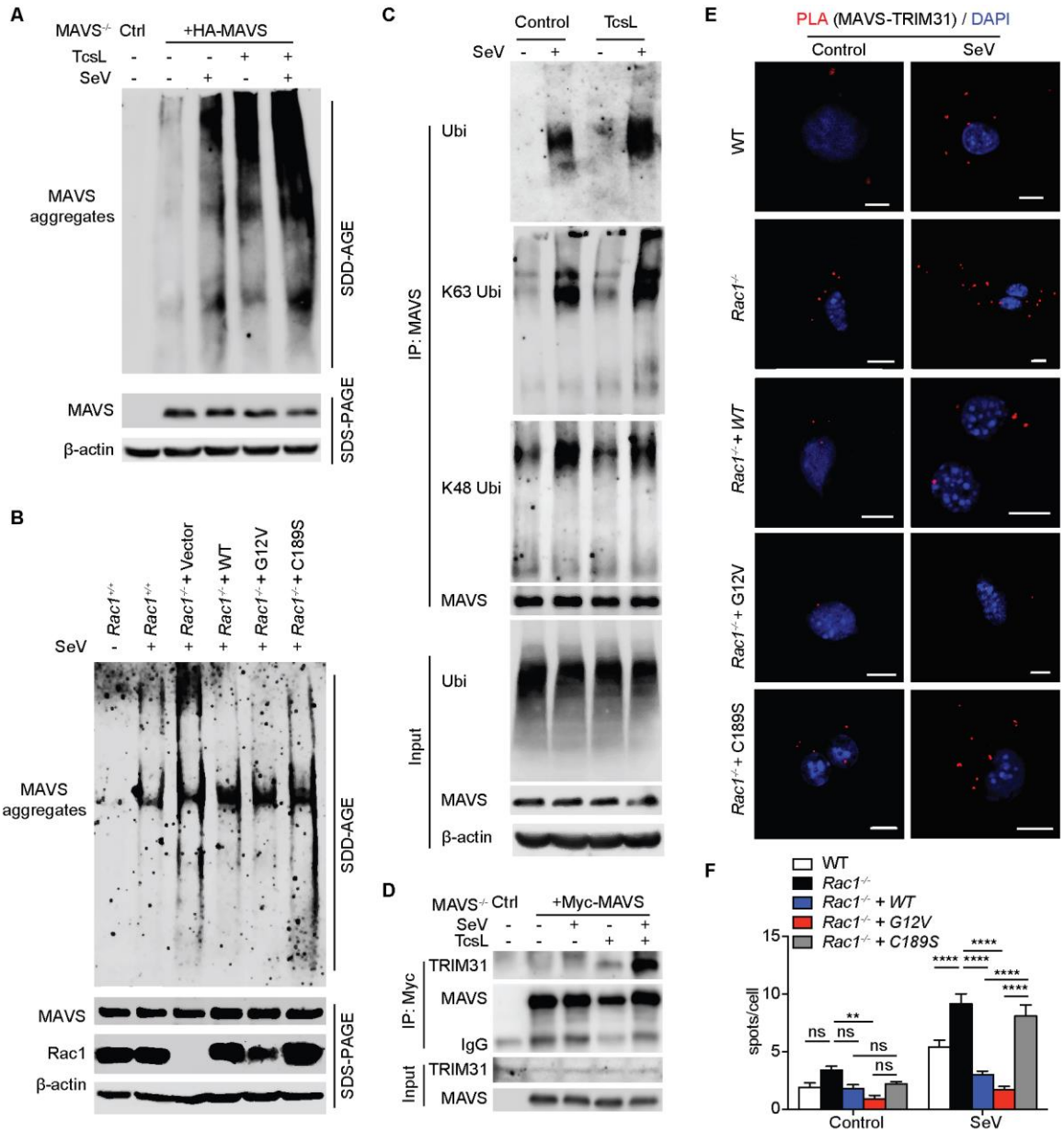
A
MAVS-/- Ctrl
+HA-MAVS
TcsL
SeV
MAVS aggregates
SDD-AGE
MAVS
β-actin
SDS-PAGE
B
Rac1+/+
Rac1+/+
Rac1-/- + Vector
Rac1-/- + WT
Rac1-/- + G12V
Rac1-/- + C189S
SeV
MAVS aggregates
SDD-AGE
MAVS
Rac1
β-actin
SDS-PAGE
C
Control
TcsL
SeV
IP: MAVS
Ubi
K63 Ubi
K48 Ubi
MAVS
Input
Ubi
MAVS
β-actin
D
MAVS-/- Ctrl
+Myc-MAVS
SeV
TcsL
IP: Myc
TRIM31
MAVS
IgG
Input
TRIM31
MAVS
E
PLA (MAVS-TRIM31) / DAPI
Control
SeV
WT
Rac1-/-
Rac1-/- + WT
Rac1-/- + G12V
Rac1-/- + C189S
F
WT
Rac1-/-
Rac1-/- + WT
Rac1-/- + G12V
Rac1-/- + C189S
spots/cell
15
10
5
0
ns
ns
**
ns
ns
****
****
****
****
****
****
Control
SeV

Figure S6

Fig. S6. MERC-localized Rac1 inhibits Trim31-MAVS interaction and subsequent MAVS Lys^{63}-linked ubiquitination, aggregation, and activation upon RNA virus infection. (**A**) Immunoblot of *Mavs*$^{-/-}$ iBMDMs reconstituted with HA-tagged *Mavs* pre-treated with TcsL, followed by infection with SeV and resolved by SDD-AGE (top) or total cell lysates resolved by SDS-PAGE (bottom). (**B**) Anti-MAVS immunoblot of mitochondria extracts of wild-type, Rac1$^{-/-}$ iBMDMs and Rac1$^{-/-}$ iBMDMs reconstituted with WT, G12V, or C189S of *Rac1*, infected with SeV for 4 h and resolved by SDD-AGE (top) or total cell lysate of iBMDMs infected with SeV resolved by SDS-PAGE (bottom). (**C**) Immunoblot with pan-ubiquitin, K63-, or K48-specific ubiquitin antibody on anti-MAVS immunoprecipitates from cell lysate of wild type macrophages pre-treated with TcsL, followed by infection with Sendai virus. (**D**) Co-immunoprecipitation analysis of the interaction of Trim31 with MAVS in *MAVS*$^{-/-}$ iBMDMs reconstituted with Myc-tagged *Mavs* pre-treated with TcsL followed by SeV infection. *Mavs*$^{-/-}$ iBMDM was used as a control. (**E** and **F**) WT or *Rac1*$^{-/-}$ iBMDMs reconstituted with WT, G12V, or C189S of *Rac1* were infected with SeV for 4 h and fixed, and endogenous MAVS and TRIM31 interaction were determined using PLA assay (red spots); Confocal images were quantified using ImageJ software, (n = 20 cells); **p: $<$ 0.01, ****p: $<$ 0.0001 (two-way ANOVA). Data are representative of three independent experiments.

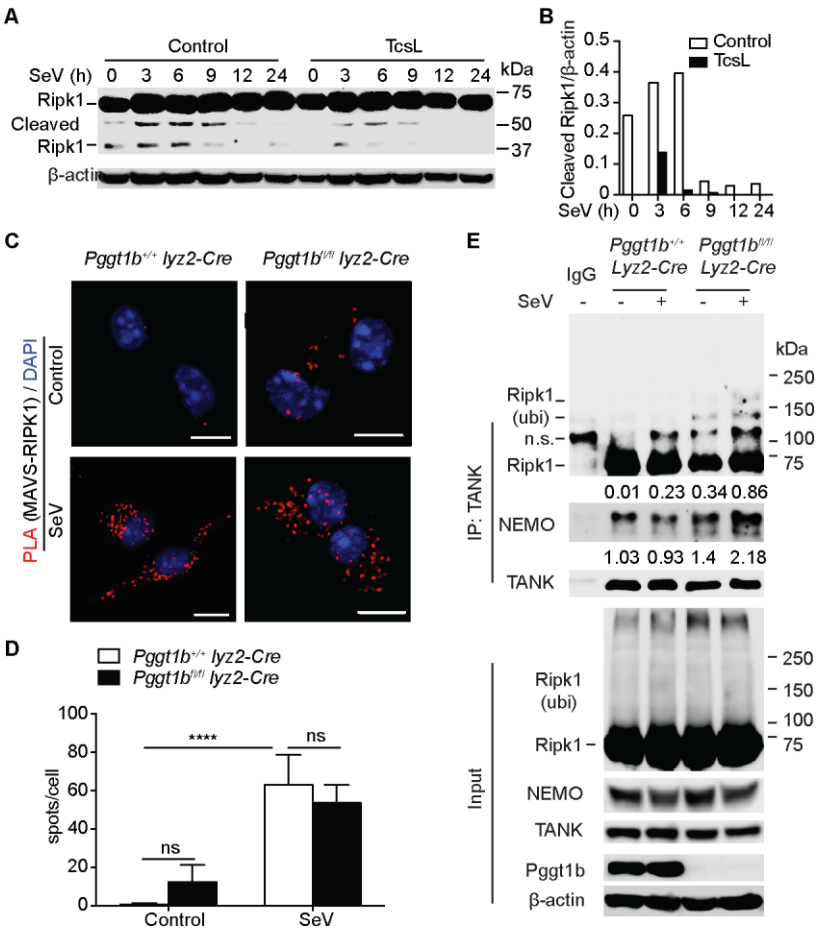
A
Control
TcsL
SeV (h) 0 3 6 9 12 24 0 3 6 9 12 24
kDa
Ripk1
Cleaved
Ripk1
β-actin
75
50
37
B
Cleaved Ripk1/β-actin
Control
TcsL
SeV (h) 0 3 6 9 12 24
C
Pggt1b+/+ lyz2-Cre
Pggt1bfl/fl lyz2-Cre
PLA (MAVS-RIPK1) / DAPI
Control
SeV
D
Pggt1b+/+ lyz2-Cre
Pggt1bfl/fl lyz2-Cre
spots/cell
****
ns
ns
Control
SeV
E
IgG
Pggt1b+/+ Lyz2-Cre
Pggt1bfl/fl Lyz2-Cre
SeV
kDa
IP: TANK
Ripk1 (ubi)
n.s.
Ripk1
0.01 0.23 0.34 0.86
NEMO
1.03 0.93 1.4 2.18
TANK
Input
Ripk1 (ubi)
Ripk1
NEMO
TANK
Pggt1b
β-actin
250
150
100
75

Figure S7

Fig. S7. MERC-localized Rac1 promotes cleavage of Ripk1 and the association of TANK with ubiquitinated Ripk1. (**A**) Immunoblot with anti-Ripk1 of cell lysate from TcsL pretreated BMDMs infected with SeV at different time points. (**B**) Densitometry of cleaved 37KD Ripk1 fragment relative to that of β-actin in the whole cell lysates (WCL) of (**A**). (**C** and **D**) *Pggt1b*$^{+/+}$ *Lyz2-Cre* and *Pggt1b*$^{fl/fl}$ *Lyz2-Cre* BMDMs were infected with SeV for 4 h and fixed, and endogenous MAVS and Ripk1 interaction were determined using PLA assay (red spots); Confocal images were quantified using ImageJ software, (n = 20 cells); ****p: ＜ 0.0001 (two-way ANOVA). (**E**) Immunoblot of anti-TANK immunoprecipitates from the total cell lysates of BMDMs infected with SeV for 4 h. Data are representative of three independent biological experiments.

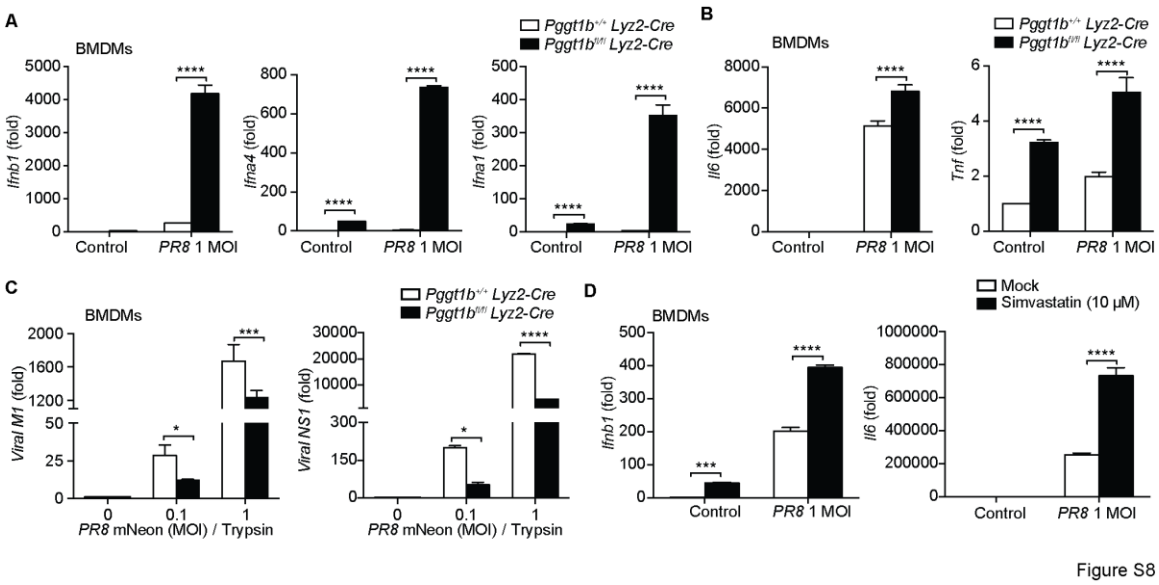

Figure S8

Fig. S8. Pggt1b deficiency and Statin pretreatment in BMDMs enhance antiviral innate immune response after influenza A virus *PR8* challenge. (**A** and **B**) Quantitative RT-PCR analysis of *Ifnb1*, *Ifna4*, *Ifna1*, *Il6 and Tnf* in BMDMs from *Pggt1b*$^{+/+}$*Lyz2-Cre or Pggt1b*$^{fl/f}$ *Lyz2-Cre* mice 9 h after acute infection with *PR8* (1 MOI). (**C**) Quantitative RT-PCR of IAV viral genes *M1* and *NS1* in BMDMs pretreated with 10 μM simvastatin for 18 h followed by infection with IAV PR8 mNeon (0.01 MOI) containing 1μg/mL TPCK-trypsin for 24 h. (**D**) Quantitative RT-PCR analysis of *Ifnb1* and *Il6* in primary BMDMs pretreated with or without 10 μM simvastatin for 18 h followed by infection with 1 MOI PR8. *p: ＜0.05, ***p: ＜0.001, ****p: ＜0.0001 (two-way ANOVA). Data are representative of three independent biological experiments.

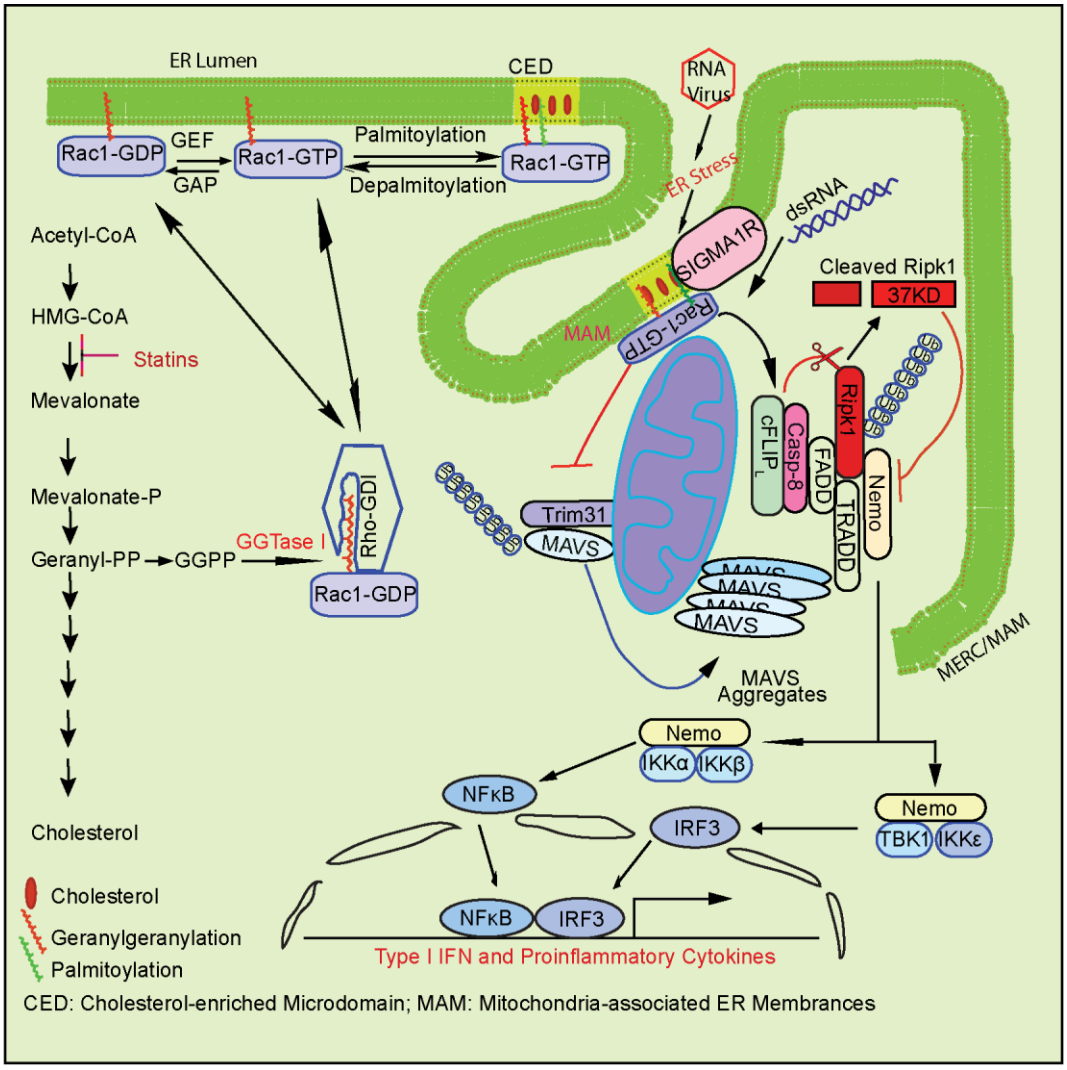

Figure S9

Fig. S9. Graphic summary.

Table S1. Primers for quantitative RT-PCR.

Gene	Forward	Reverse
mIfnb1	5'-CACAGCCCTCTCCATCAACTA-3'	5'-CATTTCCGAATGTTCGTCCT-3'
mIfna1	5'-ACCCAGCAGATCCTGAACAT-3'	5'-AATGAGTCTAGGGTATTCC-3'
mIfna4	5'-TCAAGCCATCCTTGTGCTAA-3'	5'-GTCTTTTGATGTGAAGAGGTTCAA-3'
mIl6	5'-GCTACCAAACTGGATATAATCAGGA-3'	5'-CCAGGTAGCTATGGTACTCCAGAA-3'
mTnf	5'-TGCTGGGAAGCCTAAAAGG-3'	5'-CGAATTTTGAGAAGATGATCCTG-3'
mRac1	5'-AGATGCAGGCCATCAAGTGT-3'	5'-TCAAAGACGGTGGGGATGTA-3'
mRac2	5'-GACAGTAAGCCGGTGAACCTG-3'	5'-CTGACTAGCGAGAAGCAGATG-3'
mRhoA	5'-AACTGCATCCCAGAACCTGT -3'	5'-TACCACAAGCTCCATCACCA -3'
Vrial NS1	5'-AGAAAGTGGCAGGCCCTCTTTGTA-3'	5'-TGTCCTGGAAGAGAAGGCAATGGT-3'
Vrial M1	5'-TCAGGCCCCCTCAAAGCCGA-3'	5'-GGGCACGGTGAGCGTGAACA-3'
SeV-P	5'-CAAAAGTGAGGGCGAAGGAGAA -3'	5'-CGCCCAGATCCTGAGATACAGA -3'
mPggt1b	5'CCTTCTGTGGCATTGCGTCA-3'	5'-CAACAAGGCGATCTTGAGTTG-3'
mGapdh	5'-TGGCAAAGTGGAGATTGTTGCC-3'	5'-AAGATGGTGATGGGCTTCCCG-3'
hIFNB1	5'- ATGACCAACAAGTGTCTCCTCC-3'	5'- GCTCATGGAAAGAGCTGTAGTG-3'
hIFNA1	5'-GCCTCGCCCTTTGCTTTACT-3'	5'- CTGTGGGTCTCAGGGAGATCA-3'
hGAPDH	5'- CATGAGAAGTATGACAACAGCCT-3'	5'-AGTCCTTCCACGATACCAAAGT-3'

m: murine; h: human